ORIGINAL RESEARCH

The Effects of IFN-λ on Epithelial Barrier Function Contribute to *Klebsiella pneumoniae* ST258 Pneumonia

Danielle Ahn*, Matthew Wickersham*, Sebastian Riquelme, and Alice Prince

Department of Pediatrics, Columbia University College of Physicians and Surgeons, New York, New York

ORCID ID: 0000-0002-7399-9295 (A.P.).

Abstract

IFN-λ and IL-22, cytokines that share the coreceptor IL-10RB, are both induced over the course of *Klebsiella pneumoniae* ST258 (KP35) pneumonia. IL-22 is known to protect mucosal barriers, whereas the effects of IFN-λ on the mucosa are not established. We postulated that IFN-λ plays a role in regulating the airway epithelial barrier to facilitate cellular trafficking to the site of infection. In response to IFN-λ, the transmigration of neutrophils across a polarized monolayer of airway epithelial cells was increased, consistent with diminished epithelial integrity. KP35 infection increased epithelial permeability, and pretreatment with IFN-λ amplified this effect and facilitated bacterial transmigration. These effects of IFN-λ were confirmed *in vivo*, in that mice lacking the receptor for IFN-λ ($Ifnlr1^{-/-}$) were protected from bacteremia in a murine model of KP35 pneumonia. Conversely, the integrity of the epithelial barrier was protected by IL-22, with subsequent impairment of neutrophil and bacterial transmigration *in vitro*. Maximal expression of IL-22 *in vivo* was observed later in the course of infection than IFN-λ production, with high levels of IL-22 produced by recruited immune cells at 48 hours, consistent with a role in epithelial barrier recovery. The divergent and opposing expression of these two related cytokines suggests a regulated interaction in the host response to KP35 infection. A major physiological effect of IFN-λ signaling is a decrease in epithelial barrier integrity, which facilitates immune cell recruitment but also enables *K. pneumoniae* invasion.

Keywords: airway epithelial barrier; bacterial pneumonia; IFN-λ; IL-22; *Klebsiella pneumoniae*

Clinical Relevance

Multidrug-resistant organisms such as *Klebsiella pneumoniae* are important causes of severe pneumonia with few therapeutic options. Understanding how this organism takes advantage of host signaling pathways may allow us to identify alternative ways to help the host overcome and clear this opportunistic pathogen.

Klebsiella pneumoniae ST258 has emerged as a major cause of healthcare-associated pneumonia, bacteremia, and sepsis (1, 2). Along with substantial antimicrobial drug resistance, this host-adapted pathogen has acquired mechanisms to avoid innate immune clearance pathways that are typically effective against other opportunists (3). *K. pneumoniae* clinical isolate 35 (KP35), a locally prevalent ST258 isolate, is associated with high-grade bacteremia and causes persistent infections in the airway lumen (3). This is in contrast to the highly virulent and rapidly cleared reference strain *K. pneumoniae* KPPR1 (4–6), which differs genotypically from the multidrug-resistant (MDR) isolates that are now more prevalent clinically (3). *K. pneumoniae* ST258 is also highly resistant to neutrophil-mediated phagocytosis and killing (3, 7), which undoubtedly contributes to its ability to cause persistent bloodstream infection and eventual lethality, which has been reported to be upwards of 50% (8).

Exactly how *K. pneumoniae* invades across the airway epithelium is not clearly

(Received in original form January 22, 2018; accepted in final form August 13, 2018)

*These authors contributed equally to this work.

Supported by National Institutes of Health (NIH) grants R35 HL135800 (A.P.) and NIH K08 HL138289 (D.A.). The Proteomics Core Facility is funded by NIH P30 CA013696-39S3 and the CCTI Flow Core is supported by NIH S10 RR027050.

Author Contributions: Performed experiments: D.A., M.W., and S.R. Conception and design, analysis and interpretation, and drafting of the manuscript for important intellectual content: D.A., M.W., and A.P. Responsibility for the integrity of the data and accuracy of the data analysis: all authors.

Correspondence and requests for reprints should be addressed to Alice Prince, M.D., Department of Pediatrics, Columbia University College of Physicians and Surgeons, Room 416, 650 W. 168th Street, New York, NY 10032. E-mail: asp7@columbia.edu.

This article has a data supplement, which is accessible from this issue's table of contents at www.atsjournals.org.

Am J Respir Cell Mol Biol Vol 60, Iss 2, pp 158–166, Feb 2019

Originally Published in Press as DOI: 10.1165/rcmb.2018-0021OC on September 5, 2018
Internet address: www.atsjournals.org

defined. Other opportunists that occupy a similar ecological niche, such as *Pseudomonas aeruginosa,* are motile and express type III secreted toxins (9) targeting Rho GTPAses and cytoskeletal dynamics to permit bacterial translocation (10, 11). *P. aeruginosa* also activate Ca^{2+} fluxes and calpain activity in airway epithelial cells that cleaves epithelial tight junction proteins and permits bacterial transmigration (12). However, KP35 does not stimulate Ca^{2+} release (3) and does not express a type III secreted toxin. Thus, its ability to translocate from the airway to the bloodstream so readily must be due to an alternative mechanism.

Proinflammatory cytokine signaling in response to bacterial infection promotes changes in epithelial tight junctions and facilitates the transmigration of phagocytes and other immune cells into the airway lumen in an effort to clear the pathogen. Both type I IFNs and type III IFNs (collectively referred to as IFN-λ, IFNL1, IL-28A/B, or IL-29) promote the expression of a large number of IFN-stimulated genes, many of which have proinflammatory effects (13, 14). IFN-λ signaling is mediated through receptors expressed primarily on epithelial cells, consistent with a role in mucosal infection. The type III IFNs signal through a heterodimeric receptor and share IL-10RB with IL-22. IL-22 and IFN-λ bind first to their cognate ligands, which are on adjacent loci on human chromosome 1p36.11 (15), before interacting with the common IL-10RB component (16). In a model of rotavirus infection, IL-22 and IFN-λ was shown to have synergistic effects in protecting the epithelial barrier in the gut (17). IL-22 is best characterized for its role in the production of antimicrobial peptides and in epithelial barrier defenses in the gastrointestinal tract (18). In the setting of pneumonia, IL-22 contributes to epithelial repair after influenza (19), and *Il22*$^{-/-}$ mice have a significantly increased susceptibility to severe lung injury from virulent *K. pneumoniae* infection (5).

We postulated that cytokines induced by KP35 are responsible for the changes observed in the integrity of the airway epithelial barrier, in contrast to other pathogens that do so directly. We focused on IFN-λ and IL-22 because these share a common receptor, IL10-RB, and are both involved in epithelial junctional homeostasis in the gut (17). In the experiments detailed in this report, we found that KP35 induced a brisk IFN-λ response that, in contrast to IL-22, substantially affected the integrity of the airway epithelial barrier.

Methods

Bacterial Strains and Growth Conditions

KP35 (3) and KPPR1 (ATCC 43816) were grown in Luria-Bertani and resuspended in PBS for *in vivo* and *in vitro* infections.

Cell Lines

16HBE cells, a human bronchial epithelial cell line, were used in multiple assays as described in the data supplement.

Mouse Studies

In vivo experiments were performed using age- and sex-matched cohorts of 6- to 8-week-old C57BL/6J (Jackson Laboratories), *Ifnlr1*$^{-/-}$ (Bristol-Myers Squibb), and *Il22*$^{-/-}$ (Jackson Laboratories) mice. The *Ifnlr1*$^{-/-}$ mice were acquired through a material transfer agreement with Bristol-Myers Squibb. The mice were anesthetized, infected intranasally with *K. pneumoniae* (10^8 cfu in 50 μl of PBS), and killed between 4 hours and 96 hours after infection as described previously (3) and in further detail in the data supplement. All animal experiments were performed in strict accordance with the recommendations in the "Guide for the Care and Use of Laboratory Animals" of the National Institutes of Health, the Animal Welfare Act, and U.S. federal law, as well as with the guidelines of the Institutional Animal Care and Use Committee of Columbia University (protocol numbers AAAG9307 and AAAQ8375).

Analysis of Immune Cell Populations

Analysis of cell populations in BAL fluid (BALF) was conducted using multicolor flow cytometry on a BD LSR II. Cells were labeled with a combination of fluorophores (*see* Table E1) and analyzed on FlowJo (v10.0.8) as described in the data supplement.

Bone Marrow Myeloid-derived Suppressor Cell Differentiation and Infection

Bone marrow myeloid-derived suppressor cells (BM/MDSCs) were differentiated as previously described (3) from wild-type (WT) and *Il22*$^{-/-}$ mice (for further details, *see* the data supplement).

qRT-PCR

Total RNA was isolated and measured from cultured cells and lung homogenates as described in the data supplement (Table E2).

Immunoblots

Cell lysates were studied by Western blot in the usual fashion, as described in detail in the data supplement.

Cytokine Analysis

For *in vitro* studies, supernatants were collected after 24 hours of infection with bacteria from 16HBE cells and tested via ELISA (BioLegend). For *in vivo* studies, Eve technologies measured cytokine levels by multiplex array from BALF at the indicated time points unless measuring IFN-λ (Mouse IL-28A/B) DuoSet ELISA (R&D Systems).

Dextran Permeability Assays and Transepithelial Electrical Resistance

16HBE cells were grown on Transwell Permeable Supports (Corning) filters (3-μm pore size) with an air–liquid interface. Dextran permeability and transepithelial electrical resistance assays were performed as described in detail in the data supplement.

Shotgun Proteomics

Proteomic data were obtained using methanol/chloroform precipitation, Trypsin Gold digestion (Promega), and peptide fractionation (Pierce High pH Reversed-Phase Peptide Fractionation Kit; Thermo Fisher) as previously described (3). The soluble peptide mixtures were collected for liquid chromatography tandem mass spectrometry (LC-MS/MS) analysis. We used the spectral counts from the LC-MS/MS data and applied a network analysis to a selected protein list from global proteomics expression profiling data using the ingenuity pathway analysis algorithm (QIAGEN).

Neutrophil Migration Assay

Neutrophil migration assays were performed as previously described (12) with some modifications, as described in detail in the data supplement.

Statistics

For data sets with more than two groups, multiple comparisons were analyzed using a Kruskal-Wallis nonparametric or regular one-way ANOVA with Dunn's or Dunnett's

post test, respectively. Two groups with normally distributed data were analyzed by Student's *t* test. Mouse samples were compared using the nonparametric Mann-Whitney test. Proteomic analysis was conducted using the Benjamini-Hochberg multiple comparison test. Statistical analyses were performed using GraphPad Prism software, with significance defined as $P < 0.05$.

Results

KP35 Infection Promotes Changes in Expression of Epithelial Junctional Proteins

To first understand the effects of KP35 on the airway epithelium, we performed proteomics on BALF harvested from WT mice infected with KP35 for 48 hours. Several signaling pathways related to the integrity of the epithelial junctions were affected by infection (Figure 1A). Among the most prominent pathways identified were those related to actin remodeling of epithelial adherens junctions, the actin cytoskeleton, tight and gap junctions, IL-22, IL-10, STAT3, and IFNs. Canonical epithelial remodeling and tight junction signaling pathways were differentially affected in response to KP35 (Figure 1B): several actin-related protein complexes were increased, whereas dynamins (DNM2/3) and zyxin (ZYXIN) that are involved in focal adhesion complexes (20) were downregulated. Changes in the expression of proteins directly involved in epithelial junctions were quantified over the course of KP35 infection. Significant decreases in the abundance of zonula-occludens-1 (ZO-1) and claudin-2 were apparent as early as 24 hours postinfection (hpi), whereas ezrin decreased minimally by 48 hpi and occludin levels were diminished at 96 hpi (Figure 1C). The dynamic changes in epithelial junctional protein expression were apparent with decreased ZO-1 by 48 hpi and recovery by 168 hpi, as assessed by immunofluorescence on fixed lung tissue (Figure 1D).

KP35 Induces IL-10RB Cytokines *In Vivo*

We postulated that cytokines induced by KP35 were responsible for the changes in the junctional proteins. Proteomic data indicated that IL-10RB signaling was strongly activated by KP35 (Figure 2A). Significant induction of IL-10RB at the levels of both protein expression and transcription was found in a murine model of KP35 pneumonia. Expression of IL-10RB in lung homogenate was greatest at 48 hours of infection (Figure 2B). Parallel to the expression of this receptor, IFN-λ transcription peaked at 48 hours and then declined. Conversely, IL-22 transcript levels initially decreased by 48 hours but recovered by 96 hours (Figure 2C). Total cytokine amounts in the BALF paralleled transcription, with peak cytokine levels at 48 hours for IFN-λ and 96 hours for IL-22 (Figure 2D), indicating the participation of both cytokines in the response to *K. pneumoniae* infection.

IFN-λ and IL-22 Modulate the Integrity of the Epithelial Barrier

Exactly how IFN-λ and IL-22 alter airway epithelial junctions is not well established. We used human airway epithelial cells (16HBEs) to determine how these cytokines might alter barrier function (Figure 3). The addition of IFN-λ and IL-22 to 16HBEs induced STAT signaling, the canonical pathway that is expected to be responsive to these cytokines, with phosphorylation of STAT1 and STAT3, respectively (Figure 3A). Treatment of 16HBEs with IFN-λ decreased expression of occludin and ezrin (Figure 3B), whereas IL-22 increased expression of these junctional proteins (Figure 3C). We then confirmed that the 16HBE cells responded to KP35 with significant induction of IFN-λ (*IFNL2/3*) after 24 hours, consistent with our *in vivo* model (Figure 3D).

Because peak IFN-λ levels coincided with maximal immune cell numbers in the airways (3), we postulated that IFN-λ increases barrier permeability to facilitate immune cell trafficking. We first tested the effects of IFN-λ on airway epithelial integrity by measuring the dextran permeability of polarized 16HBE monolayers exposed to both IFN-λ and KP35 (Figure 3E). IFN-λ treatment alone increased dextran permeability to the same extent that KP35 alone did, with additive effects of cytokine and bacteria stimulation together. Conversely, addition of IL-22 to the Transwell inserts significantly decreased dextran accumulation in the lower chamber of the Transwell inserts (Figure 3F), with corresponding effects on transepithelial electrical resistance (Figure 3G). Thus, exogenous IL-22 served to further enhance epithelial integrity, whereas IFN-λ increased permeability.

The physiological purposes and consequences of increased epithelial permeability include facilitating immune cell recruitment into the infected airway. Using the same Transwell system, we found that the addition of IFN-λ allowed for increased translocation of isolated neutrophils, whereas IL-22 impaired chemotaxis of neutrophils across the polarized monolayer (Figure 3H). We then assessed the effect of each cytokine on the number of bacteria that were able to transmigrate across the polarized monolayer, and observed that IFN-λ treatment increased cfu recovery across the barrier by 2 log. Again, the opposite effect was seen with IL-22 coincubation, with less recovery of bacteria in the basal compartment (Figure 3I). Therefore, an untoward effect of enhanced immune cell trafficking also enables bacteria to translocate from the airway into the lung. This is particularly relevant given that *K. pneumoniae* by itself is not motile.

Ifnlr1$^{-/-}$ Mice Are Protected from KP35 Bacteremia

The effects of IFN-λ on epithelial junctions observed in our proteomics data and analysis of epithelial barrier function *in vitro* indicated a likely contribution to KP35 invasion from the airway lumen into the bloodstream. After an intranasal inoculation of KP35, mice lacking the receptor for IFN-λ (*Ifnlr1*$^{-/-}$ mice) were significantly protected from bacteremia, as evidenced by a reduced bacterial load in the spleen, as well as fewer bacteria recovered from BALF and lungs as compared with WT mice (Figure 4A). The immune cell response to infection was similar in the WT and *Ifnlr1*$^{-/-}$ mice, with no major differences in recruitment of alveolar macrophages, granulocytic MDSCs and neutrophils, or monocytic MDSCs (M-MDSCs) (Figure 4B). The diminished bacterial load in the airways of *Ifnlr1*$^{-/-}$ mice was accompanied by significantly increased IL-22 and decreased IL-10, IL-1β, and KC/CXCL1 at 48 hours (Figure 4C). In the absence of IFN-λ receptor signaling, occludin expression remained constant over the course of infection (Figure 4D). Thus, the absence of IFNLR1 signaling enhanced KP35 clearance from the lung.

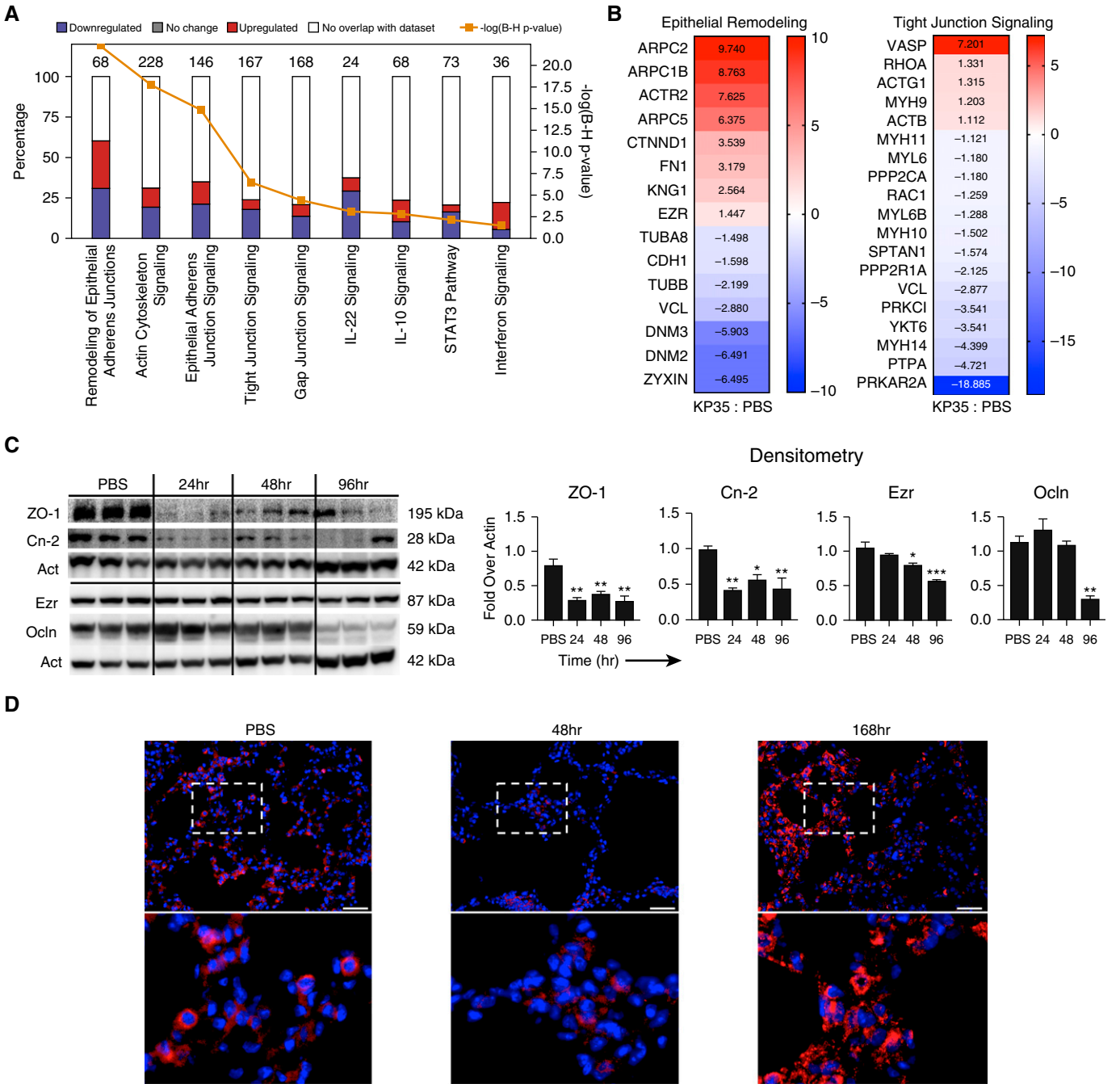

Figure 1. *Klebsiella pneumoniae* alters the expression of epithelial junctional proteins. (*A*) Ingenuity pathway analysis showing major canonical pathways significantly affected by KP35 infection of wild-type (WT) mice, using proteomic data obtained from pooled BAL fluid ($n = 3$) after 48 hours of infection. B-H = Benjamini-Hochberg. (*B*) Heatmaps of the canonical pathways of epithelial remodeling and tight junctional signaling showing relative expression of proteins in KP35-infected mice compared with PBS-treated controls. (*C*) Immunoblots of ezrin (Ezr), occludin (Ocln), zonula-occludens-1 (ZO-1), and Claudin-2 (Cn-2) from lung homogenates of WT mice infected with KP35 at the indicated time points. Densitometry values normalized to actin (Act) are shown ($n = 3$); $^{*}P < 0.05$, $^{**}P < 0.01$, $^{***}P < 0.005$; one-way ANOVA, Dunnett's *post hoc* test for multiple comparisons as compared with PBS. For all graphs, each column is the mean value ± SEM. Representative data from at least two independent experiments are shown. (*D*) Distribution of ZO-1 by immunofluorescence on nonparaffin-fixed lung sections. Lower panels represent magnification of the area defined by the white dashed line boxes in the upper panels. Scale bars: 300 μm.

IL-22 Restores Airway Epithelial Barrier Function

In contrast to the effect of IFN-λ, IL-22 increased epithelial barrier integrity *in vitro* and was upregulated late in KP35 infection, consistent with a role in the repair of the airway barrier *in vivo*. The contribution of IL-22 to the clearance of KP35 was assessed in a murine model of pneumonia, which demonstrated equivalent clearance of KP35 in the $Il22^{-/-}$ mice and WT controls (Figure 5A). WT and $Il22^{-/-}$ mice

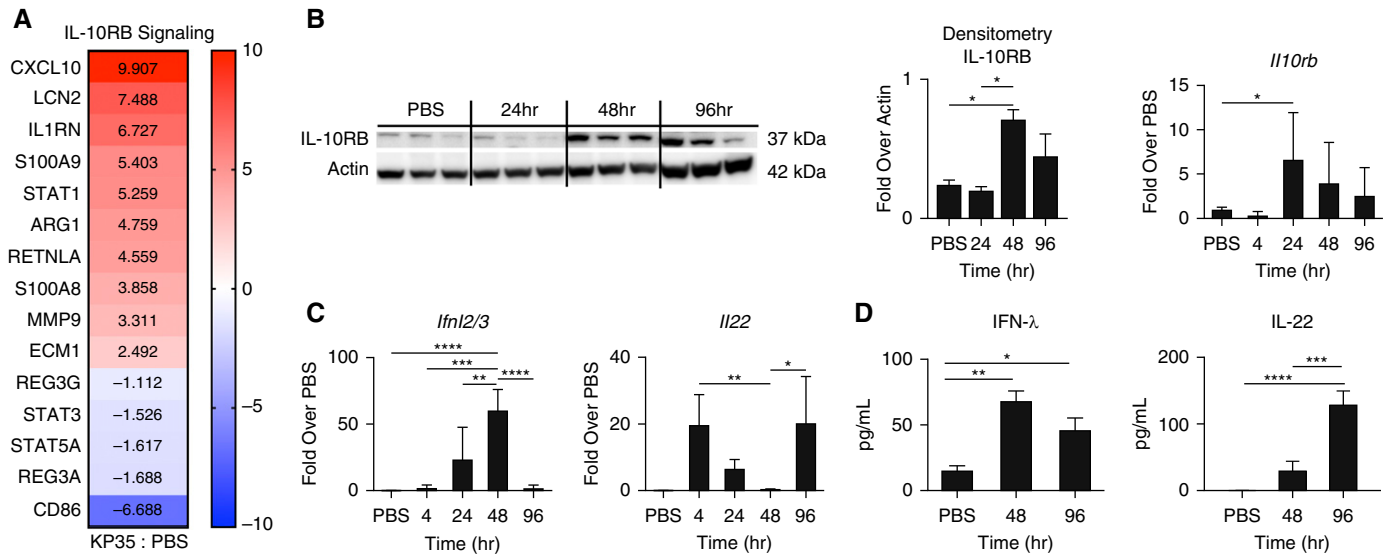

Figure 2. KP35 promotes production of the IL-10RB–related cytokines IFN-λ and IL-22. (*A*) Heatmaps of the IL-10RB signaling pathway recovered from BAL fluid of KP35-infected mice at 48 hours of infection (same samples as in Figures 1A and 1B; $n = 3$). (*B*) Immunoblot with densitometry and qRT-PCR of IL-10RB using lung homogenates of WT mice infected with KP35 at the indicated time points. (*C*) Gene expression measured via qRT-PCR of lung homogenates for IFN-λ (*Ifnl2/3*) ($n = 6$) and IL-22 (*Il22*) ($n = 6$), and (*D*) their respective protein levels measured via ELISA ($n = 3$) or multiplex array ($n = 6$) in BAL fluid from mice infected with KP35 at the indicated time points. For immunoblots, densitometry values are normalized to actin ($n = 3$). Representative data from at least two independent experiments are shown. For all graphs, each column is the mean value ± SEM. $^{*}P < 0.05$, $^{**}P < 0.01$, $^{***}P < 0.001$, and $^{****}P < 0.0001$, by one-way ANOVA; Dunnett's correction for multiple comparisons between groups indicated by the horizontal bar (*B–D*).

recruited similar numbers of immune cells, with no differences in recruitment of alveolar macrophages, granulocytic MDSCs and neutrophils, or M-MDSCs with KP35 infection (Figure 5B). The proinflammatory cytokine IL-1β was significantly increased and IL-10 production was significantly decreased at 48 hours in *Il22*$^{-/-}$ mice (Figure 5C), suggesting proinflammatory compensation in the absence of IL-22. Notably, IFN-λ was also decreased in the absence of IL-22. Thus, in contrast to the negative effects of IFN-λ on KP35 clearance, lack of IL-22 had no net consequences on KP35 clearance in the *in vivo* model.

Our findings thus far suggested a dynamic regulation of the epithelial barrier, first by the loss of barrier function associated with IFN-λ and then by production of IL-22 to restore barrier integrity. We postulated that a potential source of IL-22 is the Ly6C^{hi} monocyte (or M-MDSC) population, a major subset of immune cells that were not recruited into the airways until 48 hours after KP35 infection. These immune cells have been shown to suppress neutrophil bactericidal capacity (3) but are critical for promoting the clearance of *K. pneumoniae* (21). We found that murine BM cells differentiated into the M-MDSC phenotype (BM/MDSCs) exhibited increased production of IL-22 at the level of RNA transcription in response to KP35 infection for 4 hours (Figure 5D). At this time point, the levels of IL-22 secreted into the cell culture supernatant were similar regardless of infection. To determine the effects of MDSC-derived IL-22 on the integrity of the epithelial barrier, BM/MDSCs from WT or *Il22*$^{-/-}$ mice were exposed to KP35 and the supernatants were harvested. Addition of the sterilized MDSC supernatant from WT mice enhanced the integrity of the epithelium in that dextran translocation in response to infection was prevented, whereas supernatant derived from *Il22*$^{-/-}$ BM/MDSCs had no protective effect against dextran permeability (Figure 5E). Intracellular staining of IL-22 from cells recovered from total lung homogenate showed epithelial cells, monocytes, and neutrophils as major producers of this cytokine (Figure 5F). These results suggest that the production of IL-22 by these monocytes contributes to the restoration of airway epithelial integrity at the site of infection.

Discussion

In the experiments detailed in this report, we demonstrate the participation of the cytokines IFN-λ and IL-22 in the host defense against carbapenem-resistant *K. pneumoniae* KP35, a representative ST258 *K. pneumoniae* that is common in healthcare-associated infections. Our findings indicate that this pathogen promotes expression of IFN-λ and the IL-10RB receptor, which mediate changes in the epithelial junctions to facilitate immune cell recruitment. However, IFN-λ–induced alterations in the epithelial barrier also enable translocation of *K. pneumoniae* from the airway lumen into the lung and bloodstream. As a nonmotile organism, KP35 takes advantage of the physiological opening of epithelial tight junctions that occurs to enable neutrophil and monocyte recruitment into the airway. This is similar to the well-established mechanism of gram-negative sepsis, in which bacteria invade inflamed mucosal surfaces in the gastrointestinal tract. The ability of KP35 to achieve a high density in the airway may similarly facilitate translocation across the pulmonary mucosal barrier, leading to sepsis.

The induction of IFN-λ expression by KP35 appears to be a major factor in enabling invasion across the airway epithelial barrier. Type III IFNs have effects distinct from those of type I IFNs, targeting

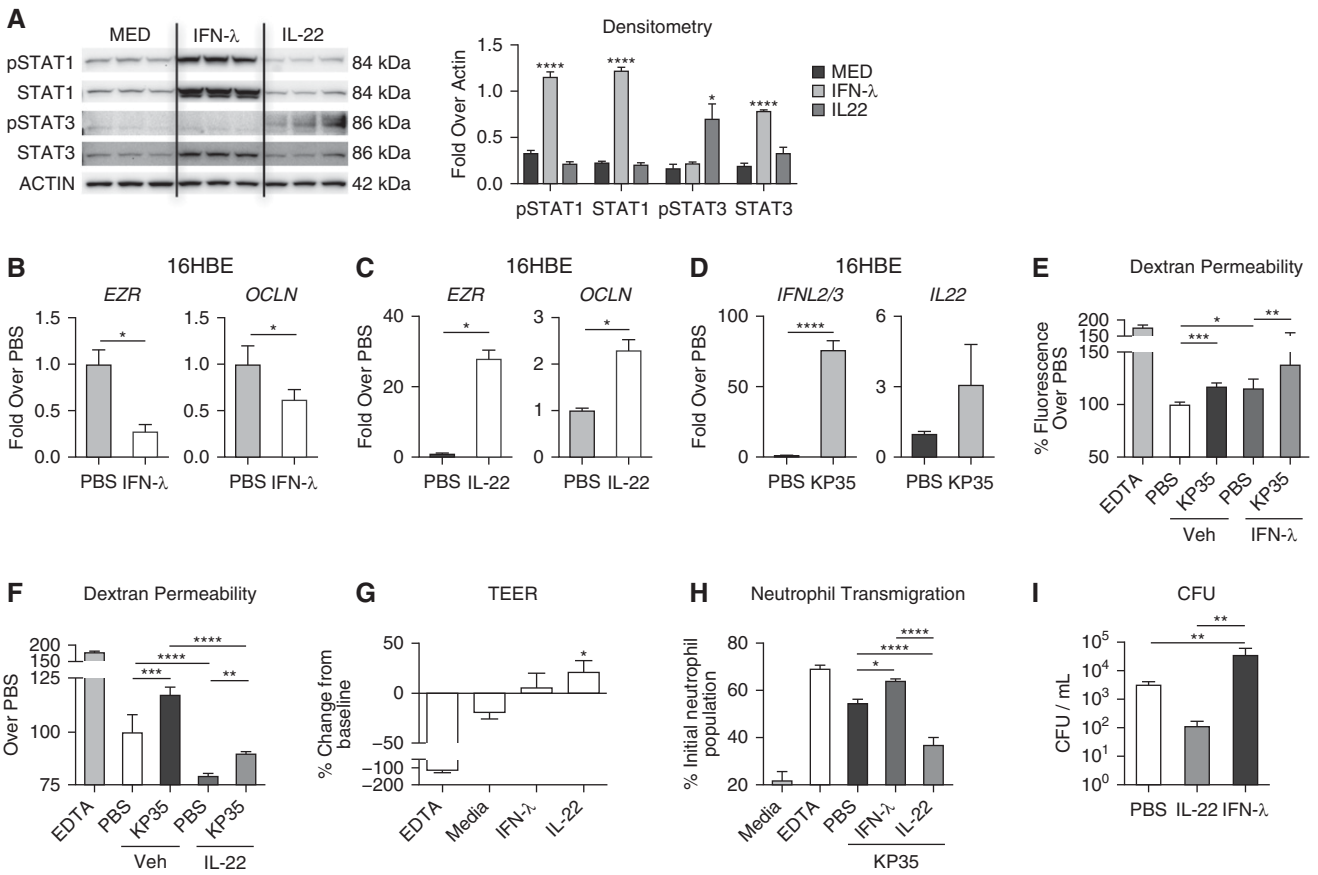

Figure 3. IFN-λ stimulates airway epithelial cells and compromises barrier integrity. (*A*) Immunoblot and densitometry of confluent human airway epithelial cells (16HBEs) stimulated with their respective cytokine for 24 hours (n = 3). (*B* and *C*) qRT-PCR of *EZR* and *OCLN* after stimulation of 16HBE cells with IFN-λ (*B*) or IL-22 (*C*) for 24 hours (n = 4). (*D*) qRT-PCR of IFN-λ (*IFNL2/3*) and IL-22 (*IL22*) (n = 5) levels in 16HBE cells after 24 hours of KP35 infection. (*E* and *F*) Dextran permeability with or without basolateral pretreatment of IFN-λ (*E*) or IL-22 (*F*) for 24 hours (n = 8, 2 compiled experiments). (*G*) The percent change in transepithelial electrical resistance (TEER) before and after treatment with IFN-λ or IL-22 for 24 hours (n = 4). (*H*) Neutrophil transmigration across polarized 16HBE cells after 4 hours of apical KP35 infection. (*I*) KP35 cfu (n = 6) recovered from the basolateral side of polarized 16HBE cells after 4 hours of apical infection with or without basolateral pretreatment of IFN-λ or IL-22 for 24 hours (n = 3). EDTA served as a positive control for transmigration assays. For column graphs, the bar is the mean value ± SEM. Representative data from at least two independent experiments are shown, unless otherwise indicated. For all graphs, each column is the mean value ± SEM. $^{*}P < 0.05$, $^{**}P < 0.01$, $^{***}P < 0.001$, and $^{****}P < 0.0001$, by Student's t test (*B–D*) or one-way ANOVA, Dunnett's *post hoc* test for multiple comparisons compared with media (MED) control (*E*, *F*, *H*, and *I*) or between the means of every other mean in other columns in the data set. Veh = vehicle.

receptors primarily displayed on epithelial cells, although they share numerous effectors (15). We found that IFN-λ suppresses transcription of occludin and ezrin, which are essential for maintaining epithelial junctional integrity. The mucosal distribution of IFNRL1 reflects a tissue-specific role in regulation of the epithelial barrier, allowing for immune cell recruitment. IFN-λ perturbation of epithelial junctions enhanced neutrophil transmigration, consistent with the function of type I and III IFNs in promoting proinflammatory responses in the respiratory tract (14). IFNRL1 is also expressed on neutrophils, with IFN-λ impairing intracellular processes such as degranulation and reactive oxygen species production (22, 23). Therefore, the added effect of IFN-λ on neutrophil function likely contributes to bacterial translocation and persistence. However, IFN-λ production alone is not sufficient to explain the persistent KP35 airway infection, as even the *Ifnlr1*$^{-/-}$ mice retained over 10^4 cfu in the airway at 96 hours, although these mice were not bacteremic at this time point.

Countering the effects of IFN-λ in KP35 infection, we observed the induction of IL-22 in the murine lung and in human human bronchial epithelial cells. The *in vitro* consequences of IL-22 on the epithelial junctions were similar to what has been proposed to occur in the gut epithelium, namely, a "tightening" of the barrier (24, 25). We demonstrate that IFN-λ and IL-22 appear to be divergently regulated, in that they are expressed at different times (IFN-λ early and IL-22 late in infection)—a coregulation that is lost in *Ifnlr*$^{-/-}$ mice. In the absence of Ifnlr, we observed an early spike in IL-22 production at 48 hours, which was absent by 96 hours. This was in contrast to the delayed kinetics of the IL-22 peak in WT mice, suggesting the potential for improved bacterial clearance with early exogenous IL-22 administration as in

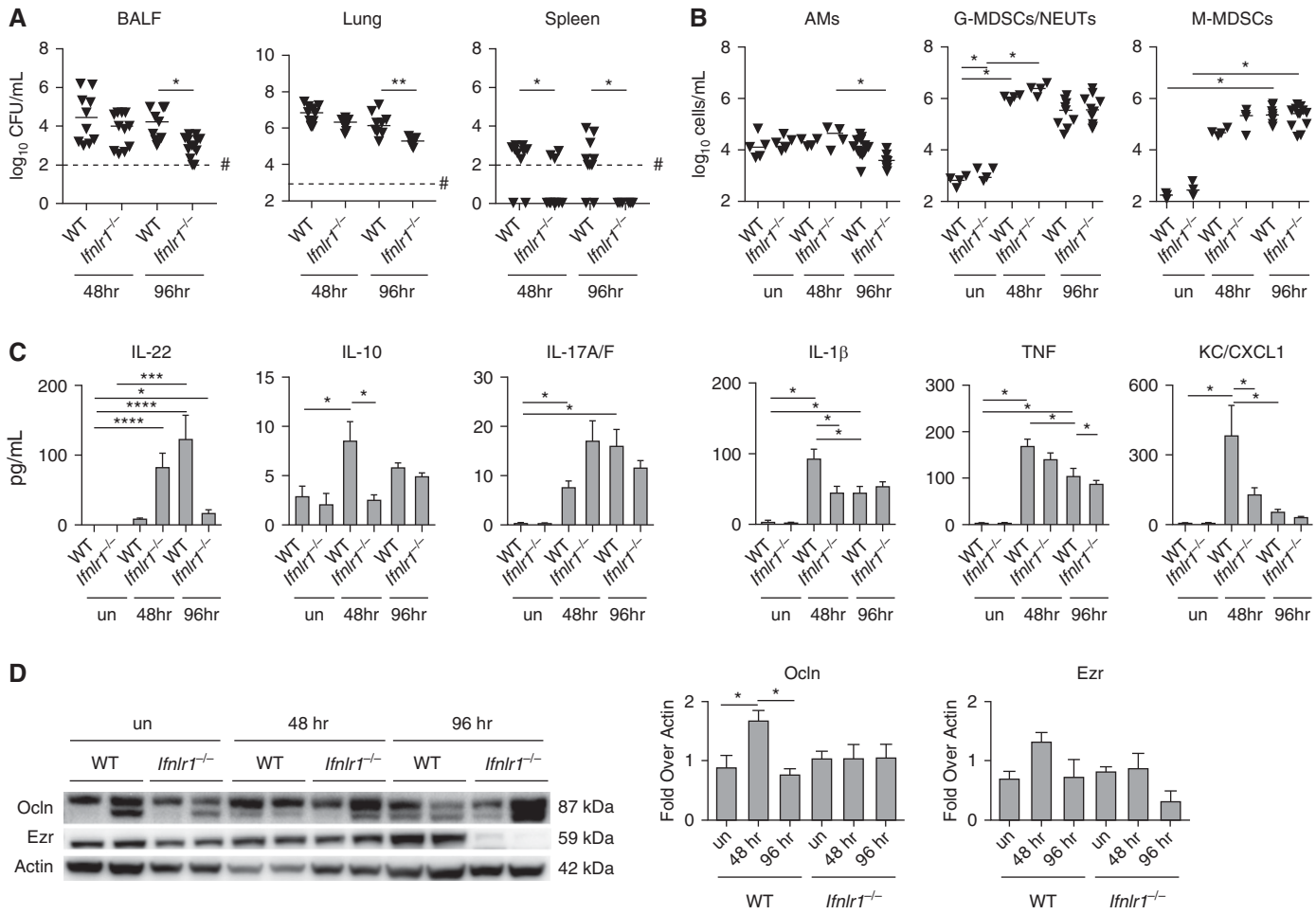

Figure 4. *Ifnlr1*$^{-/-}$ mice are protected from bacteremia. WT and *Ifnlr1*$^{-/-}$ mice were infected with KP35 for 48 or 96 hours and compared with PBS-treated controls. (*A*) Bacterial load was enumerated in BAL fluid (BALF), lung, and spleen. (*B*) Cell populations in BALF: alveolar macrophages (AMs) ($CD45^+SiglecF^+CDll11b^{lo\text{-}mid}$), granulocytic myeloid-derived suppressor cells/neutrophils (G-MDSCs/NEUTs) ($CD45^+CD11b^+MHCII^{lo}Ly6C^{hi}Ly6G^{hi}$), and monocytic myeloid-derived suppressor cells (M-MDSCs) ($CD45^+CD11b^+MHCII^{lo}Ly6C^{hi}Ly6G^{lo}$). (*C*) Cytokines in BALF (n = 8–9). (*D*) Representative immunoblot of lung homogenate for Ocln and Ezr; densitometry is the result of two experiments compiled (n = 4). For the scatter plots, each point represents an individual mouse and horizontal lines within represent median values. #Represents the limit of detection. For column graphs, the bar is the mean value ± SEM. Compiled data from at least two independent experiments are shown. Horizontal bars above the data sets equal $^*P < 0.05$, $^{**}P < 0.01$, Kruskal-Wallis test, one-way ANOVA, Dunn's correction for multiple comparisons. $^*P < 0.05$, $^{**}P < 0.01$, $^{***}P < 0.001$, and $^{****}P < 0.0001$. un = untreated.

other models of infection. The divergent kinetics of these IL-10RB cytokines was not observed for the production of the other cytokines measured. We speculate that IL-22 and IFN-λ are in some way coregulated, as the genes for their distinct receptors are adjacent on chromosome 1 and they share the use of IL-10RB. IL-10 signaling, which competes for IL-10RB, may also influence IFN-λ and IL-22 responses. However, because IL-22 and IFN-λ lead to downstream STAT3 and STAT1 signaling, respectively, this is unlikely to be a straightforward regulatory system.

Also of note was the lack of a phenotype associated with the *Il22*$^{-/-}$ mice. In KP35 infection, a major source of IL-22 appears to be the MDSC population, which dominates the myeloid response to this *K. pneumoniae* (3). Previous studies using the classic *K. pneumoniae* KPPR1 strain established a major role for IL-22 produced by natural killer cells, ILC3 cells, and T-helper cell type 17 cells (25) in preventing pulmonary damage in concert with IL-17 (5). Thus, in contrast to models of infection with organisms more susceptible to neutrophil-mediated clearance (26), IL-22 was less critical in the host response to KP35 pneumonia. We noted upregulation of the proinflammatory cytokines IL-17A/F, IL-1β, and KC/CXCL1 that appeared to compensate for the absence of IL-22–dependent signaling. Importantly, the *Il22*$^{-/-}$ mice also had decreased IFN-λ, which may have counterbalanced the effects of the two cytokines on the epithelium. Conversely, an early increase in IL-22 expression in mice lacking IFNLR1 likely helped maintain the epithelial barrier to prevent bacteremia and increase bacterial clearance.

The activation of IFN-λ and IL-22 in the host response to KP35 pneumonia

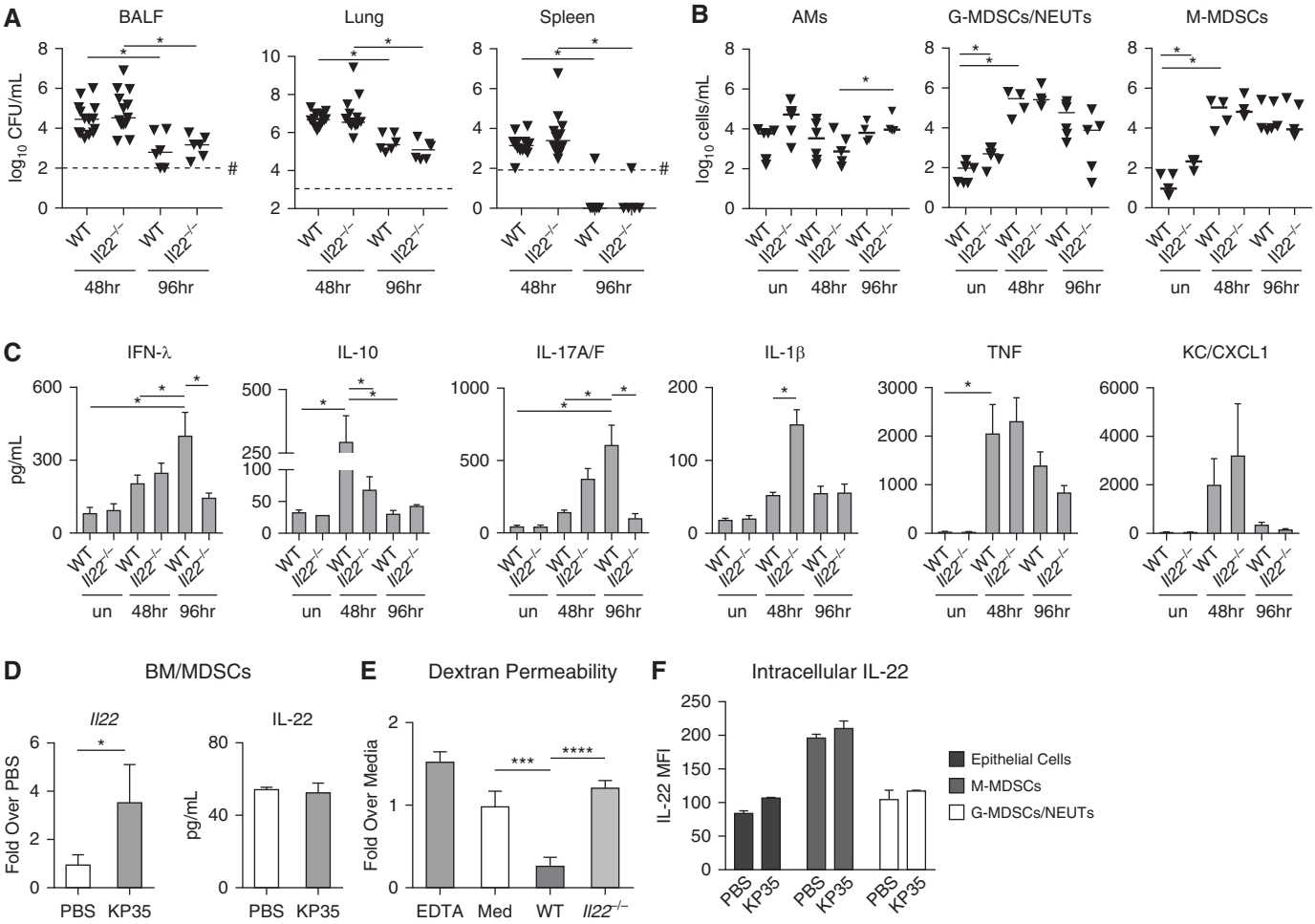

Figure 5. IL-22 increases barrier integrity during KP35 infection. (*A*) Bacterial load was enumerated in selected compartments. (*B*) Cell populations in BALF, as defined in Figure 4. (*C*) Cytokines in BALF from WT and *Il22*$^{-/-}$ mice (n = 4). (*D*) Expression of IL-22 via qRT (whole-cell lysate) and ELISA (cell culture supernatant) by BM-MDSCs infected with KP35 compared with PBS controls (n = 4). (*E*) Dextran permeability of polarized 16HBE cells with or without 24-hour pretreatment with supernatants harvested from WT or *Il22*$^{-/-}$ BM-MDSCs after 4 hours of KP35 infection. (*F*) Geometric mean fluorescence intensity of intracellular IL-22 staining of epithelial cells (Epcam^{+}CD11b^{-}), M-MDSCs, or neutrophils isolated from lung homogenate of WT mice infected for 48 hours. For scatter plots, each point represents an individual mouse and horizontal lines within represent median values. For column graphs, the bar is the mean value ± SEM. Representative data from at least two independent experiments are shown. *$P < 0.05$, ***$P < 0.005$, ****$P < 0.001$; Kruskal-Wallis test, one-way ANOVA, Dunn's correction for multiple comparisons; #represents the limit of detection. BM = bone marrow; MFI = mean fluorescence intensity.

illustrates some of the complexities and unexpected ramifications of cytokine function in pneumonia. Although these cytokines are important components of the innate immune defense, our data suggest that changes in epithelial barrier function associated with IFN-λ can also enhance KP35 dissemination from the airway lumen. The epithelial changes induced by these cytokines help to explain how organisms lacking toxin expression and motility can cause high rates of bacteremia by exploiting changes in barrier function associated with immune cell recruitment. ■

Author disclosures are available with the text of this article at www.atsjournals.org.

Acknowledgment: The authors thank Valerio Dorrello, M.D., Ph.D., at the Columbia University Medical Center for assistance in performing the immunofluorescence.

References

1. Gomez-Simmonds A, Greenman M, Sullivan SB, Tanner JP, Sowash MG, Whittier S, *et al*. Population structure of *Klebsiella pneumoniae* causing bloodstream infections at a New York City tertiary care hospital: diversification of multidrug-resistant isolates. *J Clin Microbiol* 2015;53:2060–2067.
2. Tumbarello M, Trecarichi EM, De Rosa FG, Giannella M, Giacobbe DR, Bassetti M, *et al*.; ISGRI-SITA (Italian Study Group on Resistant Infections of the Società Italiana Terapia Antinfettiva). Infections caused by KPC-producing *Klebsiella pneumoniae*: differences in therapy and mortality in a multicentre study. *J Antimicrob Chemother* 2015;70:2133–2143.

3. Ahn D, Peñaloza H, Wang Z, Wickersham M, Parker D, Patel P, *et al*. Acquired resistance to innate immune clearance promotes *Klebsiella pneumoniae* ST258 pulmonary infection. *JCI Insight* 2016;1:e89704.
4. Moore TA, Perry ML, Getsoian AG, Newstead MW, Standiford TJ. Divergent role of gamma interferon in a murine model of pulmonary versus systemic *Klebsiella pneumoniae* infection. *Infect Immun* 2002; 70:6310–6318.
5. Aujla SJ, Chan YR, Zheng M, Fei M, Askew DJ, Pociask DA, *et al*. IL-22 mediates mucosal host defense against Gram-negative bacterial pneumonia. *Nat Med* 2008;14:275–281.
6. Poe SL, Arora M, Oriss TB, Yarlagadda M, Isse K, Khare A, *et al*. STAT1-regulated lung MDSC-like cells produce IL-10 and efferocytose apoptotic neutrophils with relevance in resolution of bacterial pneumonia. *Mucosal Immunol* 2013;6:189–199.
7. Kobayashi SD, Porter AR, Dorward DW, Brinkworth AJ, Chen L, Kreiswirth BN, *et al*. Phagocytosis and killing of carbapenem-resistant ST258 *Klebsiella pneumoniae* by human neutrophils. *J Infect Dis* 2016; 213:1615–1622.
8. Munoz-Price LS, Poirel L, Bonomo RA, Schwaber MJ, Daikos GL, Cormican M, *et al*. Clinical epidemiology of the global expansion of *Klebsiella pneumoniae* carbapenemases. *Lancet Infect Dis* 2013;13: 785–796.
9. Veesenmeyer JL, Hauser AR, Lisboa T, Rello J. *Pseudomonas aeruginosa* virulence and therapy: evolving translational strategies. *Crit Care Med* 2009;37:1777–1786.
10. Soong G, Parker D, Magargee M, Prince AS. The type III toxins of *Pseudomonas aeruginosa* disrupt epithelial barrier function. *J Bacteriol* 2008;190:2814–2821.
11. Deng Q, Barbieri JT. Modulation of host cell endocytosis by the type III cytotoxin, Pseudomonas ExoS. *Traffic* 2008;9:1948–1957.
12. Chun J, Prince A. TLR2-induced calpain cleavage of epithelial junctional proteins facilitates leukocyte transmigration. *Cell Host Microbe* 2009;5:47–58.
13. Tong AJ, Liu X, Thomas BJ, Lissner MM, Baker MR, Senagolage MD, *et al*. A stringent systems approach uncovers gene-specific mechanisms regulating inflammation. *Cell* 2016;165:165–179.
14. Cohen TS, Prince AS. Bacterial pathogens activate a common inflammatory pathway through IFNλ regulation of PDCD4. *PLoS Pathog* 2013;9:e1003682.
15. Donnelly RP, Kotenko SV. Interferon-λ: a new addition to an old family. *J Interferon Cytokine Res* 2010;30:555–564.
16. Donnelly RP, Sheikh F, Kotenko SV, Dickensheets H. The expanded family of class II cytokines that share the IL-10 receptor-2 (IL-10R2) chain. *J Leukoc Biol* 2004;76:314–321.
17. Hernández PP, Mahlakoiv T, Yang I, Schwierzeck V, Nguyen N, Guendel F, *et al*. Interferon-λ and interleukin 22 act synergistically for the induction of interferon-stimulated genes and control of rotavirus infection. *Nat Immunol* 2015;16:698–707.
18. Sabat R, Ouyang W, Wolk K. Therapeutic opportunities of the IL-22-IL-22R1 system. *Nat Rev Drug Discov* 2014;13:21–38.
19. Pociask DA, Scheller EV, Mandalapu S, McHugh KJ, Enelow RI, Fattman CL, *et al*. IL-22 is essential for lung epithelial repair following influenza infection. *Am J Pathol* 2013;182:1286–1296.
20. Yoshigi M, Hoffman LM, Jensen CC, Yost HJ, Beckerle MC. Mechanical force mobilizes zyxin from focal adhesions to actin filaments and regulates cytoskeletal reinforcement. *J Cell Biol* 2005; 171:209–215.
21. Xiong H, Keith JW, Samilo DW, Carter RA, Leiner IM, Pamer EG. Innate lymphocyte/Ly6C(hi) monocyte crosstalk promotes *Klebsiella pneumoniae* clearance. *Cell* 2016;165:679–689.
22. Galani IE, Triantafyllia V, Eleminiadou EE, Koltsida O, Stavropoulos A, Manioudaki M, *et al*. Interferon-λ mediates non-redundant front-line antiviral protection against influenza virus infection without compromising host fitness. *Immunity* 2017;46:875–890.e6.
23. Broggi A, Tan Y, Granucci F, Zanoni I. IFN-λ suppresses intestinal inflammation by non-translational regulation of neutrophil function. *Nat Immunol* 2017;18:1084–1093.
24. Barthelemy A, Sencio V, Soulard D, Deruyter L, Faveeuw C, Le Goffic R, *et al*. Interleukin-22 immunotherapy during severe influenza enhances lung tissue integrity and reduces secondary bacterial systemic invasion. *Infect Immun* 2018;86:pii: e00706-17.
25. Sonnenberg GF, Fouser LA, Artis D. Border patrol: regulation of immunity, inflammation and tissue homeostasis at barrier surfaces by IL-22. *Nat Immunol* 2011;12:383–390.
26. Trevejo-Nunez G, Elsegeiny W, Conboy P, Chen K, Kolls JK. Critical role of IL-22/IL22-RA1 signaling in pneumococcal pneumonia. *J Immunol* 2016;197:1877–1883.